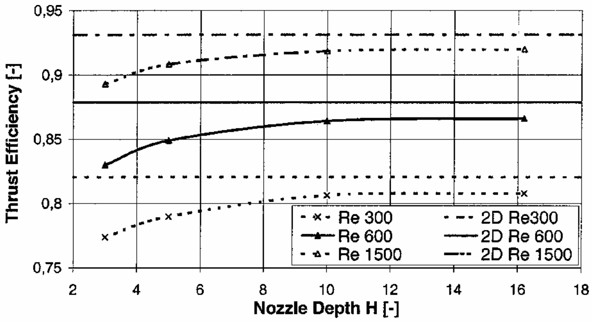

Fig. 5 Comparison of μ_{thrust} vs H for varying Re: $\epsilon = 5.4$.

Figure 4 shows the coefficient of discharge for these cases. The general trend is as expected, with an increase in throat aspect ratio leading to a solution that tends toward the two-dimensional solution as the viscous side-wall effects become less influential. Figure 5 shows a comparison between two- and three-dimensional results for throat aspect ratios and thrust efficiencies over specific Reynolds numbers. Increasing aspect ratio leads to a solution similar to that in two-dimensions. Throat aspect ratios below 10 appear to occur when three-dimensional effects are most prevalent.

Conclusions

This Note has examined the three-dimensional viscous effects in micronozzles by means of comparison with experimental data and two-dimensional computations. The main results can be summarized as follows: first, three-dimensional viscous effects are not the primary cause of divergence between two-dimensional predictions and experimental data. For the nozzle geometries examined experimentally, the throat aspect ratio is large enough so that viscous side-wall effects have little influence. Second, an examination of varying throat aspect ratios shows that increasing the aspect ratio tends to produce results similar to the two-dimensional case. A similar trend was witnessed if the Reynolds number was increased as boundary-layer effects are reduced. It was found that below an aspect ratio of around 10 three-dimensional effects begin to become significant. Third, causes for the discrepancy in thrust were examined. Spontaneous condensation was ruled unlikely. Experimental measurements of this scale are very challenging, and it is probable that the error present in the experimental work is a contributing factor to the differences with this computational work.

Acknowledgment

The authors gratefully appreciate the help of Robert L. Bayt for permission to publish experimental data.

References

[1] Bayt, R. L., Ayon, A. A., and Breuer, K. S., "A Performance Evaluation of MEMS-Based Micronozzles," AIAA Paper 97-3169, July 1997.

[2] Bayt, R. L., "Analysis, Fabrication, and Testing of a MEMS-Based Micropropulsion System," Ph.D. Dissertation, Dept. of Aeronautics and Astronautics, Massachusetts Inst. of Technology, Cambridge, MA, June 1999.

[3] Badcock, K. J., Richards, B. E., and Woodgate, M. A., "Elements of Computational Fluid Dynamics on Block Structured Grids Using Implicit Flow Solvers," *Progress in Aerospace Sciences*, Vol. 36, 2000, pp. 351–392.

W. E. Williamson
Associate Editor

Errata

Payload Deployment by Reusable Launch Vehicle Using Tether

K. D. Kumar
National Aerospace Laboratory, Tokyo 181 0015, Japan

[J. Spacecraft, 38(2), pp. 291–294 (2001)]

EQUATION (1) should be read as follows:

$$\ddot{R} = \dot{\theta}^2 R - \frac{\mu}{R^2} + \frac{3}{2}\frac{\mu}{R^2}\frac{M_e}{M}\frac{L^2}{R^2}(1 - 3\cos^2\beta\cos^2\eta)$$

$$\ddot{\theta} = -2\frac{\dot{R}}{R}\dot{\theta} + \frac{3}{2}\frac{\mu}{R^3}\frac{M_e}{M}\frac{L^2}{R^2}\sin 2\beta\cos^2\eta$$

$$\ddot{\beta} = 2\frac{\dot{R}}{R}\dot{\theta} - (\dot{\theta} + \dot{\beta})\left[(2 + \mu_c)\frac{\dot{L}}{L} - 2\dot{\eta}\tan\eta\right] - \frac{3}{2}\frac{\mu}{R^3}\left(\sin 2\beta + \frac{M_e}{M}\frac{L^2}{R^2}\sin 2\beta\cos^2\eta\right)$$

$$\ddot{\eta} = -(2 + \mu_c)\frac{\dot{L}}{L}\dot{\eta} - \frac{1}{2}(\dot{\theta} + \dot{\beta})^2\sin 2\eta - \frac{3}{2}\frac{\mu}{R^3}\cos^2\beta\sin 2\eta$$

$$\ddot{L} = \left[(\dot{\theta} + \dot{\beta})^2\cos^2\eta + \dot{\eta}^2 - \frac{\mu}{R^3}(1 - 3\cos^2\beta\cos^2\eta)\right]L + \mu_c\frac{L}{2}\left[-\frac{\dot{L}^2}{L^2} + (\dot{\theta} + \dot{\beta})^2\cos^2\eta + \dot{\eta}^2 - \frac{\mu}{R^3}(1 - 3\cos^2\beta\cos^2\eta)\right] - \frac{\text{EA}}{M_e}\varepsilon_t U(\varepsilon_t) - 2\zeta\left(\frac{\text{EA}}{M_e L_0}\right)^{\frac{1}{2}}(\dot{L} - \dot{L}_0) \tag{1}$$

where $\mu_c = (L/M_e)(\mathrm{d}M_e/\mathrm{d}L) = (1/M_e)(m_t/3M)[(m_2 + m_t/2) - 2(m_1 + m_t/2)]$.